ALEXANDER BALITSKII [*,**], *LJUBOMYR IVASKEVICH* [*], *VOLODYMYR MOCHULSKYI* [*], *JACEK ELIASZ* [**], *OLEG SKOLOZDRA* [*]

INFLUENCE OF HIGH PRESSURE AND HIGH TEMPERATURE HYDROGEN ON FRACTURE TOUGHNESS OF Ni-CONTAINING STEELS AND ALLOYS

The effect of hydrogen on short-term strength, low-cycle durability and plane-stress fracture toughness of 10Cr15Ni27 steel, 04Cr16Ni56 and 05Cr19Ni55 alloys at pressure up to 35 MPa and temperature 293...773 K was investigated. The modes of hydrogen action for which the elongation δ, reduction of area ψ, low-cycle durability N and crack resistance parameters K_c of alloys are minimal were established: hydrogen pressure above 10 MPa (non-hydrogenated specimens of 04Cr16Ni56 alloy) and above 15 MPa (hydrogenated specimens of 10Cr15Ni27 steel and 05Cr19Ni55 alloy, hydrogen concentration 15 and 19 wppm, respectively).

1. Introduction

At present, heat-resistant dispersive hardened Fe-Ni alloys are used in production of turbine blades and other parts of air-plane and rocket engines, nuclear reactors, and petrochemical equipment. In these products, heat-resistant alloys are exploited at high temperatures in contact with high-pressure hydrogen-containing gas mixtures.

It is known that age-hardened alloys are sensitive to hydrogen embrittlement [1-4]. Therefore, one of the most important requirements for such alloys is their resistance to hydrogen degradation.

In what follows, we study the influence of high-pressure gaseous hydrogen on static crack resistance, short-term strength and low-cycle durability

[*] *Karpenko Physico-Mechanical Institute, Department of Hydrogen Resistance of Materials, Naukova 5, 79601 Lviv, Ukraine; E-mail: balitski@ipm.lviv.ua, ivaskevich@ipm.lviv.ua, moculskyi@ipm.lviv.ua, skolozdra-oleg@mail.ru*

[**] *West Pomeranian University of Technology, Department of Mechanical Engeneering and Mechatronics, Piastow 19. Szczecin, 70-310, Poland; E-mail: Jacek.Eliasz@zut.edu.pl*

of 10Cr15Ni27 steel, 05Cr19Ni55 and 04Cr16Ni56 alloys in the temperature range of 293-773 K.

2. Materials and Experimental Procedure

The chemical composition, heart-treatment modes and original properties are given in Tables 1 and 2.

Table 1.

Chemical composition of steels

Alloy	Content of elements, wt.%							
	C	Cr	Ni	Mo	W	Ti	Al	Fe
10Cr15Ni27	0.09	15.18	27.1	1.41	1.9	2.85	0.29	Bal
05Cr19Ni55	0.05	19.04	Bal	8.87	-	-	1.49	12.0
04Cr16Ni56	0.04	16.4	Bal	5.24	Nb 5.2	0.58	1.0	15.1

Table 2.

Modes of thermal treatment and mechanical properties of steels in helium/hydrogen (35 MPa) at room temperature

Alloy	Thermal treatment		Mechanical properties			
	Solution treatment	Mode of aging	$\sigma_{u,}$ MPa	$\sigma_{ws0,2}$ MPa	δ %	ψ %
10Cr15Ni27	1373K, 1 h	1023K, 16 h	1270	870	17	23
		923K, 10 h	1240	880	15	20
05Cr19Ni55	1323K, 1 h	1000K, 15 h	1080	650	35	38
		923K, 10 h	970	660	7	21
04Cr16Ni56	1373K, 1 h	1023K, 16 h	1320	840	34	48
		923K, 10 h	880	750	4	12

Static tensile tests were carried out on standard five-fold cylindrical specimens (Fig. 1a) by displacement rate V = 0.1 mm/mm. During the test, the specimen was positioned in the chamber (Fig. 2a) specially designed for high-temperature tests at 293-1093 K temperature range under 0.1-35 MPa hydrogen pressure. The specimens were tested in 293-1073 K temperature range under 35 MPa hydrogen pressure and, as a comparison, in helium.

The low-cycle durability for pure strain-controlled sign-preserving bending was found under pressures of 35MPa for the amplitudes ε = 1.6% and a loading frequency of 0.5 Hz on polished plane specimens with a working part of 3×6×15 mm (Fig. 1b). The stress intensity factor under static loading K_c was computed either for the maximum force F_c in the "F-V" linear diagram or for the force F_Q determined by using the 5% secant for nonlinear diagrams [5]. Rectangular compact specimens 50×60×20 mm in
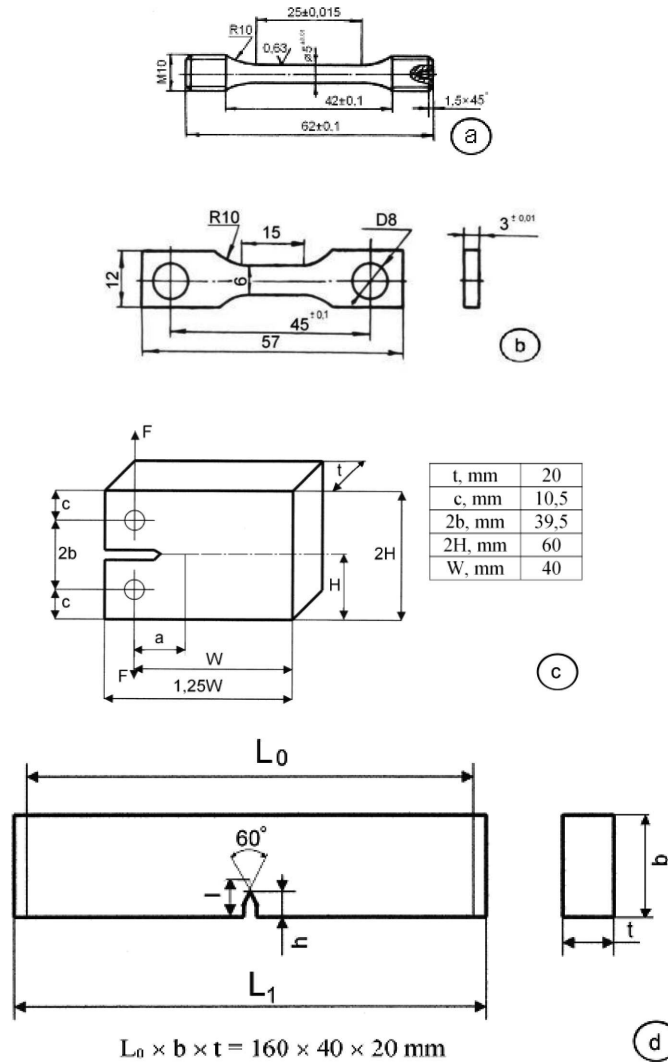
Fig. 1. Specimens for tensile testing (a), low cycle durability (b), static (c) and cyclic crack resistance (d)

size (Fig. 1c) were tested for eccentric tension in a high-pressure chamber under pressures of 0.4-30 MPa at a strain rate of 0.1 mm/min. The values of K_c can be found by using the Srawley-Gross formula [6]. The cyclic crack resistance (CCR) characteristics were determined in three-point bending of 160x40x20 mm beam (Fig. 1d) specimens at a frequency of loading of 20 Hz and a coefficient of cycle asymmetry R = 0.22 [6]. A fatigue crack 2 mm long was preliminarily grown from a stress concentrator. We placed specimens with a crack in a high-pressure chamber, set on EUS-40 unit, where, upon attaining required parameters of the hydrogen atmosphere, loaded them
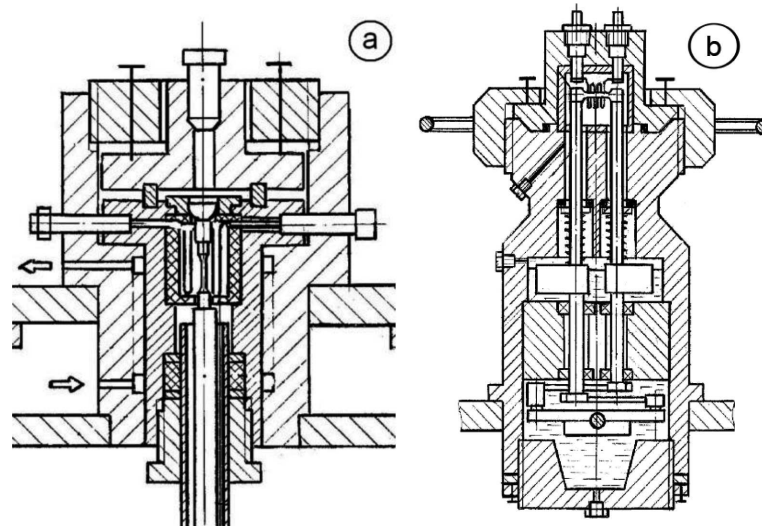
Fig. 2. Scheme of equipments for tensile testing (a) and testing of low cycle durability (b)

according to a known technique, we determined the threshold ΔK_{th} in hydrogen. The lengths of cracks were measured by changing the parameters of the electromagnetic eddy field. Transducers were preliminarily calibrated in air by comparing changes in eddy currents caused by the growth of a crack with the changes in the length of cracks measured optically on a specimen with a KM-8 cathetometer. We constructed kinetic fatigue fracture diagrams (KFFD) in helium and hydrogen under pressures up to 10 MPa at temperatures of 293 to 673 K based on experimentally obtained lengths of cracks Δl during ΔN cycles under a load F*.

To determine the indicated mechanical characteristics in hydrogen, the working chambers were preliminarily evacuated, blown-out with hydrogen, again evacuated, and filled with hydrogen up to a given pressure. At high temperatures, the specimens were held under the testing conditions for 30 min. It has been established [2, 4] that, at some values of hydrogen pressure and strain rate, which depended on the chemical compositions and structures of materials, one obtains maximum influences of hydrogen on the plasticity, low-cycle fatigue life, and static and cyclic crack resistance of martensitic steels and nickel alloys. In short-term tension, austenitic dispersion-hardened steels are substantially embrittled by hydrogen after preliminary hydrogenation at elevated temperatures and upon attaining its content above 12 ppm, and the properties of hydrogenation specimens at room temperature in air and hydrogen are equal [1, 2]. This is why we held a part of the specimens for 10 h in a hydrogen atmosphere under 623 K and 35 MPa. These regimes provide hydrogenation of specimens to the hydrogen contents of 15 wppm in

10Cr15Ni27 steel, 19 and 20 wppm in 05Cr19Ni55 and 04Cr16Ni56 alloys, respectively. Hydrogenated and non-hydrogenated specimens were tested in helium and hydrogen under different pressures. The hydrogen content in iron-nickel alloys was determined with a LECO TCH 600 instrument, typical hydrogen desorption intensity curves are shown in Fig. 3.
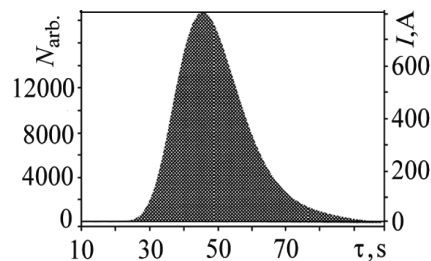

Fig. 3. Intensity of hydrogen desorption from the specimen (tigel current) in the function of exposition time (hydrogenation 673 K; 10 MPa; 10 h, common quantity of desorbed hydrogen – 6.5 ppm)

3. Experimental results

3.1. Influence of hydrogen pressure on the mechanical properties

In the cases of 04Cr16Ni56 alloy, the dependence of low-cycle durability (N), the plasticity parameters (δ and ψ) (Fig. 4-6) and plane-stress fracture toughness (K_c) (Fig. 7, curves 5, 6) on the hydrogen pressure consists of two regions. In the first region (low pressures), the parameters N, δ, ψ and K_c drop abruptly, and in the second, the negative influence of hydrogen is practically independent of pressure (Fig. 4-7). This means that there exists a pressure which causes the limiting degradation of materials properties. An additional effect of preliminary dissolved hydrogen (C_H = 20 wppm) on the properties of 04Cr16Ni56 alloy was manifested at hydrogen environment pressure less than 10 MPa.

The parameters of loading and the modes of hydrogen action for which the mechanical characteristics of the 04Cr16Ni56 alloy take minimal values at 293 K can be formulated as follows:

– the strain rate V = 0,1 mm/min ($6.7 \cdot 10^{-5}$ s^{-1}) at short-term static tension and static crack propagation;

– the frequency and amplitude of bending under the conditions of low-cycle fatigue are ν = 0, 5 Hz and ε = 1.6% respectively, and the pressure of hydrogen must be higher than 10 MPa.

In the case of 10Cr15Ni27 steel and 05Cr19Ni55 alloy, the low-cycle durability N, plasticity parameters δ and ψ (Fig. 4, 5, curves 1, 3, 5) and
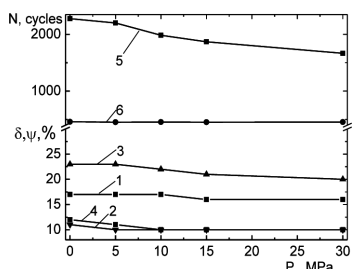
Fig. 4. Relative elongation δ (1, 2), reduction of area ψ (3, 4) (V = 0,1 mm/min.) and number cycles to failure N (5, 6) (ε = 1,6%)for specimens of 10Cr15Ni27 steel versus hydrogen pressure P at 293 K: 1, 3, 5 – non-hydrogenated specimens; 2, 4, 6 – hydrogenated specimens
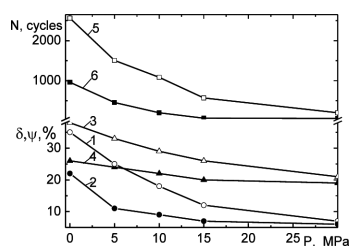
Fig. 5. Relative elongation δ (1, 2), reduction of area ψ (3, 4) (V = 0,1 mm/min.) and number cycles to failure N (5, 6) (ε = 1,6%) for specimens of 05Cr19Ni55 alloys versus hydrogen pressure P at 293 K: 1, 3, 5 – non-hydrogenated specimens; 2, 4, 6 – hydrogenated specimens
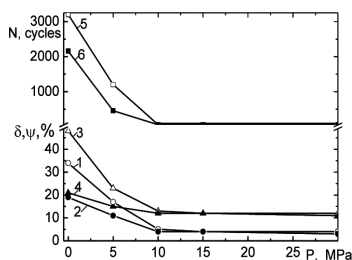
Fig. 6. Rrelative elongation δ (1, 2), reduction of area ψ (3, 4) (V = 0,1 mm/min.) and number cycles to failure N (5, 6) (ε = 1,6%) for specimens of 04Cr16Ni56 alloys versus hydrogen pressure P at 293 K: 1, 3, 5 – non-hydrogenated specimens; 2, 4, 6 – hydrogenated specimens

plane-stress fracture toughness K_c (Fig. 7, curve 1, 3) decrease in the whole hydrogen pressure range. The preliminary dissolved hydrogen (C_H = 15 wppm and 19 wppm respectively) causes a considerable additional decrease in the properties of this materials (Fig. 4, 5, curves 2, 4, 6; Fig. 7, curve 2, 4).

Thus, to estimate the serviceability of alloy 04Cr16Ni56, it is enough to test the specimens in gaseous hydrogen, while for steel 10Cr15Ni27 and alloy 05Cr19Ni55 there is a need for preliminarily hydrogenation.
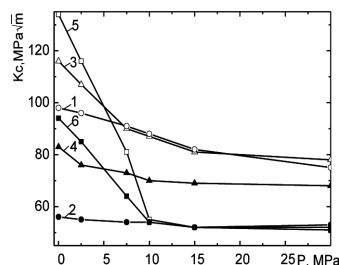
Fig. 7. Fracture toughness K_c of 10Cr15Ni27 steel (1, 2) 05Cr19Ni55 (3, 4) and 04Cr16Ni56 (5, 6) alloys versus hydrogen pressure P at 293 K: 1, 2, 5 – non-hydrogenated specimens; 3, 4, 6 – hydrogenated specimens

3.2. Influence of temperature on the static crack resistance in hydrogen

The character of influence of the temperature on 10Cr15Ni27 steel fracture toughness depends of on their conditions (Fig. 8). When temperature increases, the crack resistance in helium first rises from 98 (293 K) to 120 MPa (423 K) and, in the range 423-693 K, minimally changes (curve 1); in this case, the thickness of the specimens is insufficient for the realization of the plane strained state. Gaseous hydrogen reduces noticeably the crack resistance even at room temperature, and this effect becomes dramatically stronger as the temperature increases to 423 K (curve 2). In the range of rather low temperature, the influence of preliminary hydrogenation prevails, and, at 423 K, the crack resistances in hydrogen of preliminarily hydrogenated (curve 3) and non-hydrogenated (curve 2) specimens are equal, i.e., at this temperature, a sufficient amount of hydrogen penetrates into the material from the gas phase even during the experiment. As the temperature further rises, the negative influence of hydrogen is weakened in the absence of difference in the values of K_c between the hydrogenated and non-hydrogenated specimens, but, even at a maximum temperature, the parameter K_c in hydrogen is 21% smaller than that in helium.

The additional effect of preliminary hydrogenation on the parameter of static growth resistance K_c for the alloy 05Cr19Ni55 is appreciable only at room temperature (Fig. 9, curves 2, 3). At 373 K, the value of K_c for hydrogenated and non-hydrogenated specimens are almost equal, i.e., this temperature is sufficient for hydrogenation of dispersion-hardening nickel base alloys from the hydrogen atmosphere. For all loading modes, the degree and temperature interval of hydrogen degradation for alloy 04Cr16Ni56 is much larger than for alloy 05Cr19Ni55 (Fig. 9).

The plane-strain condition required for the evaluation of K_{Ic} were fulfilled on compact tension specimens made of alloy 04Cr16Ni56 with a thickness of 20 mm at hydrogen pressure above 10 MPa in the temperature range of 293-473 K. Fracture toughness K_c for alloy 05Cr19Ni55 decreased at 293 K

from 116 MPa in helium to 78 MPa in hydrogen under the pressure of 30 MPa, and to 68 MPa in hydrogen under the pressure of 30 MPa after preliminary high-temperature hydrogenation (with hydrogen concentration 19 wppm). The plane-strain conditions were not fulfilled in these two cases.
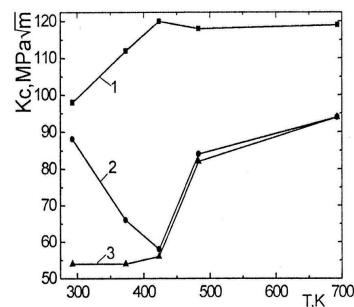

Fig. 8. Temperature dependence of static stress intensity factor K_c of 10Cr15Ni27 steel in helium (1), in hydrogen under pressure 10 MPa (2) and in hydrogen under pressure 10 MPa after hydrogenation (673 K; 10 MPa; 10 h.) (3)
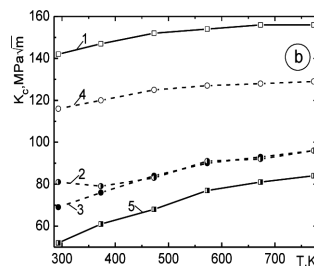

Fig. 9. Temperature dependence of static stress intensity factor K_c of 05Cr19Ni55 (2-4) and 04Cr16Ni56 (1, 6) alloys in helium (1, 4), in hydrogen under pressure 10 MPa (2, 5) and in hydrogen under pressure 10 MPa after hydrogenation (673 K; 10 MPa; 10 h.) (3)

At static crack resistance tests, a substantial difference in the character of fracture was observed in the whole temperature range 293-773 K investigated (Fig. 10a-d).

In a neutral atmosphere, there appeared a transgranular fracture with a dimple microrelief, precipitations on the bottom of dimples, and an insignificant number of individual intergranular cracks (Fig. 10a, c). In hydrogenated specimens, in regions near the front of a fatigue crack, facets of intergranular fracture and regions of quasicleavage with combs of break-off along boundaries carbide-matrix and intermetallic compound-matrix dominated (Fig. 10b). The combs of break-off indicated the localization of plastic deformation in thin regions where microcracks were initiated by quasicleavage on the boundary of the γ and γ – phases. In individual regions of fracture with a plane surface with steps, spalling in a fee lattice was detected. This

was caused by the simultaneous propagation of a crack in several crystallographic planes within the boundaries of one grain. In the region of shear lips, hydrogen substantially reduces the fraction and sizes of nonequilibrium dimples and increases the fraction of intergranular cleavage (Fig. 10c, d).
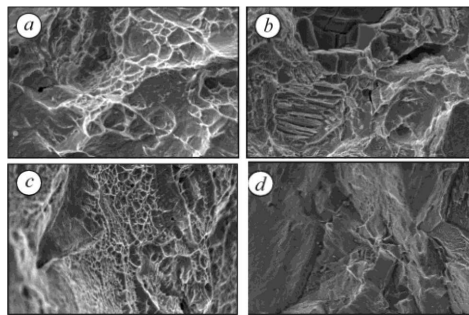

Fig. 10. Fracture surface of 10X15H27T3B2MP steel at the crack front (*a*, *b*) and shearing jaws
(*c*, *d*) at static loading at 673 K (*a*, *b*) in helium (*a*, *c*) and in hydrogen under the pressure
10 MPa after hydrogenation (623 K; 10 MPa; 10 h) (*b*, *d*). ×3000

4. Conclusions

The parameters of loading and the modes of hydrogen action for which the mechanical characteristics of the investigated alloys take minimal values at room temperature can be formulated as follows:

– strain rate V $\leq 6.7 \cdot 10^{-5}$ s^{-1} for tensile test and the strain amplitude $\varepsilon = 1.6$ % under the conditions of low-cycle fatigue at hydrogen pressures above 10 MPa for the alloy 04Cr16Ni56 and hydrogen pressures above 15 MPa at concentration of preabsorbed hydrogen and 19 wppm for the alloy 05Cr19Ni55;

– for static crack propagation at hydrogen pressure above 10 MPa for the alloy 04Cr16Ni56 and hydrogen pressure above 15 MPa at concentration of absorbed hydrogen 15 wppm for the steel 10Cr15Ni27 and 19 wppm for the alloy 05Cr19Ni55.

The plane-strain conditions required for the evaluation of K$_{Ic}$ were fulfilled on compact tension specimens made of alloy 04Cr16Ni56 with thickness of 20 mm at hydrogen pressure above 10 MPa in the temperature range 293-473 K.

Substantial difference in the fracture toughness values and in the character of fracture of all investigated materials was observed in the whole temperature range 293-773 K. In a neutral atmosphere, fracture is ductile, dimple with an insignificant number of intergranular microcracks, whereas in hydrogen, facets of intergranular fracture and regions of quasicleavage

with combs of break-off along boundaries carbide-matrix and intermetallic compound-matrix dominate.

REFERENCES

[1] Balitskii A.I., and Panasyuk V.V.: "Workability assessment of structural steels of power plant units in hydrogen environments," Probl. Prochn., No. 1, 69-75 (2009).

[2] Balitkii A.I., Ivaskevich L.M., Mochulskyi V.M.: Temperature Dependences of Age-Hardening Austenitic Steels Mechanical Properties in Gaseous Hydrogen. In: Proceedings on CD ROM of the 12th International Conference on Fracture, Ottawa, Canada, July 12-17, 2009).- Edited by M. Elboujdaini.- Ottawa: NRC.-2009.- Paper No T19.001. -7 p.

[3] Moody N.R., and Greulish F.A.: Hydrogen indused slip band fracture in Fe-Ni-Co superalloy // Scr. Metallurgica. - 1985. - **19**. - p. 1107-1116.

[4] Thompson A.W., and Bernstein L.M.: "The role of metallurgical variable in hydrogen-assisted environmental fracture," in: M.G. Fontana and R.W. Staehle (editors), Advances in Corrosion Science and Technology, Plenum, New York (1980).

[5] COST 25506-85. Methods for Mechanical Testing of Metals. Determination of the Characteristics of Crack Resistance (Fracture Toughness) Under Static Loading [in Russian], Izd. Standartov, Moscow (1985).

[6] Brown W.F., and Srawley J.E.: Plane Strain Crack Toughness Testing of High Strength Metallic Materials, ASTM Publ., No. 410 (1966).

Wpływ wodoru wysokiego ciśnienia i temperatury na ciągliwość stali niklowych i stopów Ni

S t r e s z c z e n i e

W ramach przeprowadzonych badań określono wpływ wodoru na krótkotrwałą wytrzymałość i płasko-naprężeniową ciągliwość stali 10Cr15Ni27 oraz stopów niklu 04Cr16Ni56, 05Cr19Ni55 przy wielkościach ciśnienia do 35 MPa i zakresie temperatury od 293 do 773 K. Wpływ wodoru wysokiego ciśnienia powoduje, że wydłużenie, plastyczność, wytrzymałość nisko cyklowa N i parametr odporności na pękanie K_c przyjmują minimalne wartości dla próbek stopu 04Cr16Ni56 przy ciśnieniu wynoszącym 10 MPa, natomiast dla nasyconych wodorem próbek stali 10Cr15Ni27 i stopu 05Cr19Ni55 minimum wartości tych parametrów występuje przy ciśnieniu 15 MPa, dla koncentracji wodoru wynoszącej odpowiednio 15 i 19 wppm.